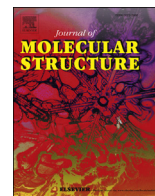




Since January 2020 Elsevier has created a COVID-19 resource centre with free information in English and Mandarin on the novel coronavirus COVID-19. The COVID-19 resource centre is hosted on Elsevier Connect, the company's public news and information website.

Elsevier hereby grants permission to make all its COVID-19-related research that is available on the COVID-19 resource centre - including this research content - immediately available in PubMed Central and other publicly funded repositories, such as the WHO COVID database with rights for unrestricted research re-use and analyses in any form or by any means with acknowledgement of the original source. These permissions are granted for free by Elsevier for as long as the COVID-19 resource centre remains active.



# The molecular structure of 4-methylpyridine-N-oxide: Gas-phase electron diffraction and quantum chemical calculations

Natalya V. Belova<sup>a,\*</sup>, Georgiy V. Girichev<sup>a</sup>, Vitaliya E. Kotova<sup>a</sup>, Kseniya A. Korolkova<sup>a</sup>,  
Nguyen Hoang Trang<sup>b</sup>

<sup>a</sup> Ivanovo State University of Chemistry and Technology, Research Institute for Thermodynamics and Kinetics of Chemical Processes, 153460 Ivanovo, Russia

<sup>b</sup> Vietnam National University, Hanoi, Vietnam

## ARTICLE INFO

### Article history:

Received 6 November 2017

Accepted 16 November 2017

Available online 17 November 2017

### Keywords:

4-methylpyridine-N-oxide

Gas-phase electron diffraction

Quantum chemical calculations

Molecular structure

NBO analysis

## ABSTRACT

The molecular structure of 4-methylpyridine-N-oxide, 4-MePyO, has been studied by gas-phase electron diffraction monitored by mass spectrometry (GED/MS) and quantum chemical (DFT) calculations. Both, quantum chemistry and GED analyses resulted in  $C_s$  molecular symmetry with the planar pyridine ring. Obtained molecular parameters confirm the hyperconjugation in the pyridine ring and the  $sp^2$  hybridization concept of the nitrogen and carbon atoms in the ring. The experimental geometric parameters are in a good agreement with the parameters for non-substituted N-oxide and reproduced very closely by DFT calculations. The presence of the electron-donating  $CH_3$  substituent in 4-MePyO leads to a decrease of the ipso-angle and to an increase of  $r(N \rightarrow O)$  in comparison with the non-substituted PyO. Electron density distribution analysis has been performed in terms of natural bond orbitals (NBO) scheme. The nature of the semipolar  $N \rightarrow O$  bond is discussed.

© 2017 Elsevier B.V. All rights reserved.

## 1. Introduction

The considerable interest to the heterocyclic compounds containing N-oxide group is caused by their pronounced biological activity [1]. Among the representatives of this class, there are compounds with bactericidal, analgesic, anticonvulsant activity, as well as ones with apoptotic, antifungal and antimicrobial activity [2,3]. These properties allow to use N-oxides as inhibitor of HIV-1 reverse transcriptase [4,5], as antiviral agent against various SARS coronavirus strains [6], and as antiadhesive and quorum-sensitive inhibitor [7]. In the literature one can find the evidence, that some complexes with pyridine-N-oxides are used in agriculture to regulate plant growth rates [8]. It was shown that pyridine-N-oxide derivatives are genotoxic [9]. The biochemical activity of N-oxides is usually considered to be the result of complexation with the metalloporphyrins in living organisms [10–12]. The reactivity of N-oxides may vary due to different substituents in the ring [13]. The variation of the substituents gives wide possibilities to chemical modifications of N-oxides and allows to influence their complexing properties, and, as the result, their biological activity. To

understand the complexation ability of N-oxides with different substituents the detailed information about the properties of free molecules is needed.

The available literature data about molecular structure of N-oxides can not be considered comprehensive. Thus, only pyridine-N-oxide and three of its para-substituted compounds have been studied by gas-electron diffraction (GED) [14,15]. Analyzing the average values of bond lengths in the pyridine ring the authors of [15] have concluded that the aromaticity increases in the series: 4-nitropyridine-N-oxide (4-NO<sub>2</sub>PyO), 4-chloropyridine-N-oxide (4-ClPyO), pyridine-N-oxide (PyO), 4-methylpyridine-N-oxide (4-MePyO). The crystal structures of PyO, 4-NO<sub>2</sub>PyO and 4-MePyO have been studied by X-ray crystallography [16,17]. The quantum chemical study of the substituent effect on the properties of pyridine-N-oxides has been performed for ten compounds with different substituents [18]. The comparative analysis of structural data obtained by different methods suggests that the molecular parameters of N-oxides obtained by GED [15] look rather strange. Thus, the N–C bond lengths in 4-NO<sub>2</sub>PyO, 4-MePyO, 4-ClPyO recommended in Ref. [15] are even longer than  $r(C-C)$  in benzene ring, and seems to be overestimated compare to the calculated values and X-ray data. Moreover, the bond distance  $r(N \rightarrow O)$  in 4-MePyO molecule recommended by authors [15] appears to be significantly overestimated and conflicting with the calculated and X-ray

\* Corresponding author.

E-mail address: [belova@isuct.ru](mailto:belova@isuct.ru) (N.V. Belova).

values. Furthermore, the accuracy of GED data obtained in Refs. [14,15] cannot be considered today as satisfactory.

The discrepancies in molecular structure of substituted N-oxides according to GED and other methods motivated us to perform a new gas-electron diffraction study of 4-methylpyridine-N-oxide. This molecule has been chosen because of the largest structural contradictions. Now more sophisticated methods for the analysis of GED data are available, including the possibility of quantum chemical results to be used in the interpretation of experimental data. This allows us to determine the structural parameters more precisely compared to the studies performed in 1982.

## 2. Experimental part

The electron diffraction patterns and the mass spectra were recorded simultaneously using the techniques described previously [19,20]. Two series of GED/MS experiments at two different nozzle-to-plate distances were performed. The conditions of GED/MS experiments and the relative abundance of the characteristic ions of 4-MePyO are shown in Tables 1 and 2, respectively. The temperature of stainless steel effusion cell was measured by a W/Re-5/20 thermocouple, which was standardised using the melting points of Sn and Al. Polycrystalline ZnO was used to establish the wavelength of the fast electrons. Microphotometric measurements were carried out by means of automatic techniques [32]. The molecular intensities were obtained in the ranges  $2.5\text{--}28.7 \text{ \AA}^{-1}$  (short camera) and  $1.3\text{--}15.5 \text{ \AA}^{-1}$  (long camera). The molecular intensities and the radial distributing curves are shown in Figs. 2 and 3 respectively.

## 3. Quantum chemical calculation

Quantum chemical calculations were carried out with GAUSSIAN 03 program set [21]. A hybrid DFT computational methods, namely B3LYP [22–26] and PBE0 [27], as well as MP2 method, were used. Structure optimizations were followed by calculations of the vibrational frequencies in order to ensure that a minimum on the potential energy hyper-surface had been reached.

Analysis of the potential functions of methyl group internal rotation shows that there is only one stable geometric configuration with H5C6C1C2 about  $90^\circ$  (see Fig. 1 for atom numbering). Although it should be noted that the internal rotation barrier is negligibly small, 0.007 kcal/mol (B3LYP/cc-pVTZ) or 0.03 kcal/mol (MP2/cc-pVTZ), thus the rotation of CH<sub>3</sub> group in 4-MePyO can be considered as free.

The geometrical parameters of the calculated equilibrium structure are listed in Table 3. Vibrational amplitudes and corrections,  $\Delta r = r_{h1} - r_a$ , were derived from theoretical force fields (B3LYP/cc-pVTZ) by Sipachev's method (approximation with taking into account the nonlinear kinematic effects at the level of the first order perturbation theory for the transformation of Cartesian coordinates into internal coordinates), using the program SHRINK [28–30]. Relevant values are listed in Table 4 (excluding nonbonded distances involving hydrogen).

**Table 1**  
The conditions of GED/MS experiment.

nozzle-to-plate distance, mm	338	598
fast electron beam, $\mu\text{A}$	1.86	0.83
temperature of effusion cell, K	371(5)	372(5)
accelerating voltage, kV	82.2	81.9
(electron wavelength), $\text{\AA}$	0.04119(3)	0.04124(4)
ionization voltage, V	50(1)	50(1)
exposure time, s	135	120
residual gas pressure, Torr	$1.9 \cdot 10^{-6}$	$3.3 \cdot 10^{-6}$
s-values range, $\text{\AA}^{-1}$	2.5–28.7	1.3–15.5

**Table 2**  
Mass spectral data recorded simultaneously with GED data for 4-methyl-pyridine-N-oxide ( $U_{\text{ioniz}} = 50 \text{ V}$ ).

m/e	Ion	Relative abundance, I, %
109	$[\text{M}^a]^+$	100
94	$[\text{M} - \text{CH}_3]^+$	29
78	$[\text{M} - \text{CH}_3 - \text{O}]^+$	14
66	$[\text{C}_4\text{H}_4\text{N}]^+$	25
52	$[\text{C}_4\text{H}_4]^+$	54

<sup>a</sup>  $\text{M} = \text{C}_6\text{H}_7\text{NO}$ .

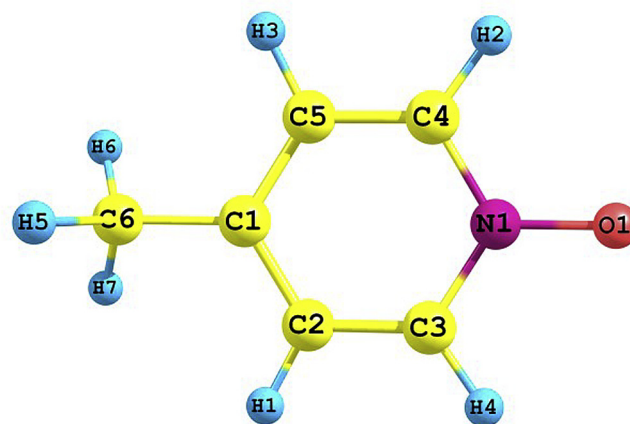


**Fig. 1.** Molecular structure of 4-methyl-pyridine-N-oxide and atom notations.

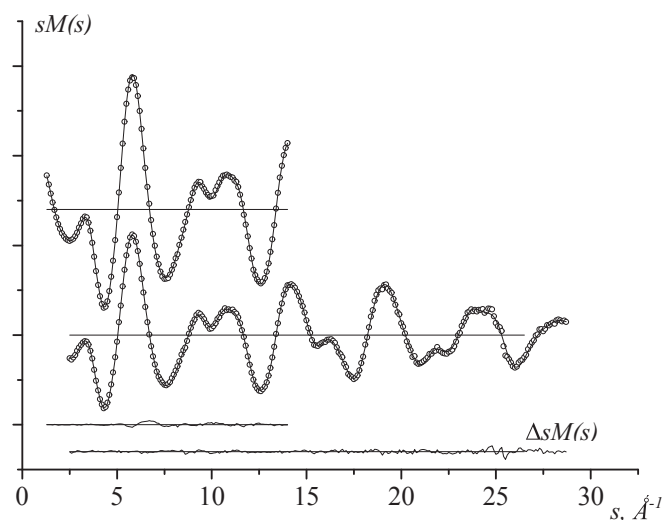


**Fig. 2.** Experimental (dots) and theoretical (solid) molecular intensity curves for 4-MePyO and the difference (experimental – theoretical) at two nozzle-to-plate distances,  $L_1 = 598 \text{ mm}$  and  $L_2 = 338 \text{ mm}$ .

The NBO 5G program [31], implemented for natural orbital analysis in PC GAMESS [32], was used to obtain the net atomic charges, and to study the effect of hyperconjugation on the structure. B3LYP/aug-cc-pVTZ wave functions were used in the NBO analyses. Relevant values of net atomic charges, Wiberg bond indexes, and second order interaction energies ( $E^{(2)}$ ) between donor-acceptor orbitals are collected in Tables 6 and 7.

Visualization of the natural orbitals performed by the ChemCraft program [33].

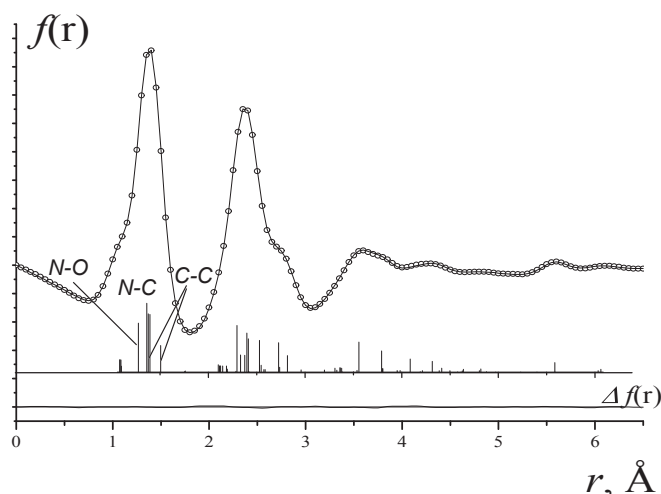


Fig. 3. Experimental (dots) and theoretical (solid) radial distribution curves for 4-MePyO and the difference curve (experimental – theoretical).

#### 4. Structure analysis

The heaviest ion in the mass spectrum observed during the GED/MS experiment was  $[\text{Me-PyO}]^+$  (Table 2). No ions were detected, which could arise from impurities. This proves the monomeric vapour composition under the conditions of the GED experiment.

The theoretical  $sM(s)$  functions were calculated with the following assumptions. Independent  $r_{h1}$  parameters were used to describe the molecular structure. Starting parameters from B3LYP/cc-pVTZ calculations were refined. The differences between all C–C, as well as between all C–H bond lengths were constrained to calculated values (B3LYP/cc-pVTZ). In compliance with the quantum chemical calculation results, a planar skeleton with  $C_{2v}$  symmetry of the pyridine ring was assumed. The methyl group was considered in the framework of  $C_{3v}$  symmetry. Vibrational amplitudes were refined in groups with fixed differences. With the abovementioned assumptions, four bond distances and four bond angles (Table 3) were refined simultaneously with six groups of vibrational amplitudes. Vibrational amplitudes were refined in

groups with fixed differences (Table 4). Only two correlation coefficients had absolute values larger than 0.7:  $(r(\text{N-C3})/r(\text{C2-C3})) = -0.74$ , and  $(\angle \text{NC3C2})/(\angle \text{C3NC4}) = -0.84$ . The best agreement factor is  $R_f = 3.4\%$ . Final results of the least squares analysis are given in Table 3 (geometric parameters) and Table 4 (vibrational amplitudes).

#### 5. Results and discussion

Table 3 summarizes the structural parameters of 4-Me-PyO. We can note a perfect agreement between calculated and experimental molecular structure parameters. The molecule possesses almost  $C_s$  symmetry (the torsional angle H5C6C1C2 is close to  $90^\circ$ ) with the planar pyridine ring. Table 5 compares gas-phase structures of PyO and 4-Me-PyO obtained in Refs. [14,15] and in this work. The parameters obtained in our research is in a good agreement with the theoretical results (therein and [18]) and, also, with the parameters for non-substituted N-oxide in contrast to the values recommended by Chiang J. F. et al. [15]. Furthermore, the parameters of free molecules of PyO [14] and 4-Me-PyO obtained in this work are in a good agreement with the crystal structures [34,35]. Apparently, some increase of the semipolar N→O bond lengths in the crystal phase compared to free molecules is due to intermolecular hydrogen bonding. All parameters presented in Table 5 confirm the hyperconjugation in the pyridine ring and the  $sp^2$  hybridization concept of the nitrogen and carbon atoms in the ring. The exceptions are only the data by Chiang J. F. et al. [15], which look rather strange.

Unfortunately, the correct comparison of GED parameters of 4-MePyO and non-substituted pyridine-N-oxide looks to be impossible because of large uncertainties in GED values obtained for PyO [14]. According to quantum chemical calculations the insertion of the methyl group in *para* – position to the PyO has no significant effect on the structural parameters of the pyridine ring, excluding only the *ipso*-angle  $\angle \text{C2C1C5}$ , which changes from  $120.6^\circ$  in PyO to  $115.9^\circ$  in 4-MePyO (B3LYP/cc-pVTZ). It is interesting to note, that the substituent effects on the geometry of heterocyclic ring are rather similar to the tendencies for the benzene ring [36,37]. Thus, the presence of the electron-donating  $\text{CH}_3$  substituent leads to the decrease of the *ipso*-angle. Furthermore, according to the calculations the  $r(\text{N} \rightarrow \text{O})$  bond lengths appear to be also sensitive to a

Table 3  
Experimental and calculated geometric parameters of 4-methyl-pyridine-N-oxide.<sup>a</sup>

	$(r_{h1}, \angle_{h1})^b$	$(r_e, \angle_e)$ B3LYP/cc-pVTZ	$(r_e, \angle_e)$ PBE0/cc-pVTZ	$(r_e, \angle_e)$ MP2/cc-pVTZ
$r(\text{N-O})$	1.275(3) $p1^c$	1.274	1.262	1.256
$r(\text{N-C3})$	1.364(3) $p2$	1.367	1.361	1.378
$r(\text{C2-C3})$	1.379(3) $p3$	1.377	1.374	1.379
$r(\text{C1-C2})$	1.397(3) ( $p3$ )	1.395	1.391	1.396
$r(\text{C1-C6})$	1.505(3) ( $p3$ )	1.503	1.496	1.500
$r(\text{C3-H4})$	1.084(3) $p4$	1.078	1.079	1.078
$r(\text{C2-H1})$	1.088(3) ( $p4$ )	1.082	1.084	1.082
$r(\text{C6-H5})$	1.099(3) ( $p4$ )	1.093	1.094	1.091
$r(\text{C6-H6})$	1.096(3) ( $p4$ )	1.090 <sup>d</sup>	1.091 <sup>d</sup>	1.089 <sup>d</sup>
$\angle \text{C3NC4}$	117.7(8) $p5$	117.9	117.7	117.5
$\angle \text{NC3C2}$	122.1(8) $p6$	121.5	121.7	121.4
$\angle \text{C3C2C1}$	120.8(6)	121.6	121.6	122.0
$\angle \text{C2C1C5}$	116.6(6)	115.9	115.8	115.7
$\angle \text{C1C6H5}$	108.6(5) $p7$	111.2	111.1	111.2
$\angle \text{C1C6H6}$	108.6(5) ( $p7$ )	111.4 <sup>d</sup>	111.3 <sup>d</sup>	111.1 <sup>d</sup>
$\angle \text{H6C6H5}$	110.4(7)	107.3 <sup>d</sup>	107.3 <sup>d</sup>	107.6 <sup>d</sup>
H5C6C1C2	87.6(69) $p8$	89.9	89.4	89.2

<sup>a</sup> Distances in Å and angles in degrees. For atom numbering see Fig. 1.

<sup>b</sup> Uncertainties in  $r_{h1}$   $\sigma = (\sigma_{sc}^2 + (2.5\sigma_{LS})^2)^{1/2}$  ( $\sigma_{sc} = 0.002r$ ,  $\sigma_{LS}$  – standard deviation in least-squares refinement), for angles  $\sigma = 3\sigma_{LS}$ .

<sup>c</sup>  $p_i$  – parameter refined independently. ( $p_i$ ) – parameters calculated from the independent parameter  $p_i$  by a difference  $\Delta = p_i - (p_i)$  from the quantum chemical calculations (B3LYP/cc-pVTZ).

<sup>d</sup> Average value.

**Table 4**

Root-mean-square vibrational amplitudes and vibrational corrections for 4-methyl-pyridine-N-oxide calculated from the molecular force field. Interatomic distances and vibrational amplitudes obtained from the GED refinements.<sup>a</sup>

	$r_{hi}^b$	$l(GED)^c$	$b_{calc}^b$ (B <sup>L</sup> LYP)	$r_{h1-r3}$ (B3LYP)
C3–H4	1.084(3)	0.070(2) <i>l</i> <sup>d</sup>	0.075	0.0016
C4–H2	1.084(3)	0.070(2) <i>l</i>	0.075	0.0017
C2–H1	1.088(3)	0.070(2) <i>l</i>	0.076	0.0015
C5–H3	1.088(3)	0.070(2) <i>l</i>	0.076	0.0015
C6–H5	1.099(3)	0.074(2) <i>l</i>	0.079	0.0008
C6–H7	1.096(3)	0.073(2) <i>l</i>	0.078	–0.00002
C6–H6	1.096(3)	0.073(2) <i>l</i>	0.078	0.0003
N–O	1.275(3)	0.037(2) <i>l</i>	0.042	0.0006
N–C3	1.364(3)	0.043(2) <i>l</i>	0.049	0.0011
N–C4	1.364(3)	0.043(2) <i>l</i>	0.049	0.0004
C4–C5	1.379(3)	0.043(2) <i>l</i>	0.048	0.0010
C2–C3	1.379(3)	0.043(2) <i>l</i>	0.048	–0.00008
C1–C2	1.397(3)	0.044(2) <i>l</i>	0.049	0.0014
C1–C5	1.397(3)	0.044(2) <i>l</i>	0.049	–0.0002
C1–C6	1.505(3)	0.045(2) <i>l</i>	0.051	0.00003
O...C4	2.299(5)	0.042(8) <i>l</i>	0.057	0.0043
O...C3	2.299(5)	0.042(8) <i>l</i>	0.057	0.0018
C3...C4	2.334(6)	0.040(8) <i>l</i>	0.055	0.0018
C2...C5	2.377(6)	0.040(8) <i>l</i>	0.056	0.0022
N...C2	2.400(5)	0.038(8) <i>l</i>	0.054	0.002
N...C6	2.400(5)	0.038(8) <i>l</i>	0.054	0.0019
C1...C4	2.414(5)	0.039(8) <i>l</i>	0.054	0.0014
C1...C3	2.414(5)	0.039(8) <i>l</i>	0.054	0.0013
C5...C6	2.535(5)	0.055(8) <i>l</i>	0.070	0.0066
C2...C6	2.535(5)	0.055(8) <i>l</i>	0.070	0.0022
C2...C4	2.730(6)	0.055(9) <i>l</i>	0.062	0.0030
C3...C5	2.730(6)	0.055(9) <i>l</i>	0.062	0.0024
N...C1	2.819(7)	0.054(9) <i>l</i>	0.060	0.0024
O...C5	3.564(7)	0.064(5) <i>l</i>	0.060	0.0070
O...C2	3.564(7)	0.064(5) <i>l</i>	0.060	0.0047
C4...C6	3.802(8)	0.075(5) <i>l</i>	0.072	0.0092
C3...C6	3.802(8)	0.075(5) <i>l</i>	0.072	0.0053
O...C1	4.094(9)	0.068(10) <i>l</i>	0.062	0.0066
N...C6	4.324(9)	0.073(10) <i>l</i>	0.067	0.0085
O...C6	5.599(12)	0.079(16) <i>l</i>	0.069	0.0144

<sup>a</sup> Values in Å, atom numbering are shown in Fig. 1.

<sup>b</sup> Uncertainties in  $r_{hi}$ – distances are  $\sigma = (\sigma_{sc}^2 + (2.5\sigma_{LS})^2)^{1/2}$  ( $\sigma_{sc} = 0.002r$ ,  $\sigma_{LS}$ –standard deviation in least-squares refinement).

<sup>c</sup> Uncertainties for amplitudes are  $\sigma = 3\sigma_{LS}$ .

<sup>d</sup> Group number of amplitude.

substituent nature. Thus, the presence of the electron donating methyl group results in an increase of  $r(N \rightarrow O)$ .

The calculated Wiberg bond indexes along with the net atomic charges for PyO and 4-MePyO are summarized in Table 6. The C–C and C–N bond orders in the ring for both molecules, as well as the

**Table 6**

Net atomic charges (q, e) and Wiberg bond indexes according to NBO scheme (B3LYP/aug-cc-pVTZ).

	PyO	4-Me-PyO
q(O)	–0.512	–0.539
q(N)	0.099	0.082
q(C3)	–0.023	–0.004
q(C2)	–0.208	–0.211
q(C1)	–0.220	–0.026
q(C6)		–0.599
Q(N–O)	1.308	1.271
Q(N–C3)	1.190	1.203
Q(C3–C2)	1.488	1.485
Q(C2–C1)	1.411	1.382
Q(C1–C6)		1.040

**Table 7**

Relevant second order perturbation energies  $E^{(2)}$  (donor – acceptor), kcal/mol (B3LYP/aug-cc-pVTZ).

Donor	Acceptor	$E^{(2)}$	
		PyO	4-Me-PyO
$\pi(C1-C2)$	$\pi^*(C3-N)$	30.9	33.4
$\pi(C1-C2)$	$\pi^*(C4-C5)$	21.7	20.4
$\pi(C4-C5)$	$\pi^*(C1-C2)$	16.7	18.4
$\pi(C4-C5)$	$\pi^*(C3-N)$	14.9	14.6
Lp(2) O	$\sigma^*(C3-N)$	11.5	10.1
Lp(3) O	$\pi^*(C3-N)$	64.3	55.5

values of the distances from Tables 3 and 5 show that these bonds do not correspond to either single nor double bonds. This confirms the existence of  $\pi$ -conjugation in the pyridine rings. The C1–C6 bond order for 4-MePyO corresponds to the single C–C bond. It is interesting to note that Q(N–O) in both molecules can not be interpreted as exact single or double bond. Moreover, the introduction of an electron-donating substituent increases the bond length N→O, slightly reduces the corresponding bond order and significantly increases the electron density on the oxygen. One can conclude that in this case the nucleophilic properties of the molecule increase. Furthermore, as it has been mentioned previously [18] the introduction of electron-donating substituents to the heterocyclic ring of N-oxides results in increasing ability for complex formation. Our experimental and calculated data (Tables 3, 6 and 7) reveal the incorrectness of the authors of [15] in their conclusion about more single N–O bond character in 4-MePyO.

The delocalization of electron density between occupied Lewis

**Table 5**

Molecular parameters of PyO and 4-MePyO (Å, deg.).

	4-MePyO			PyO			
	GED [15]	GED [this work]	X-ray [34]	B3LYP/cc-pVTZ	GED [14]	X-ray [35]	B3LYP/cc-pVTZ
r(N–O)	1.405	1.275(3)	1.309	1.274	1.290(15)	1.305	1.271
r(N–C3)	1.430(33)	1.364(3)	1.342	1.367	1.384(11)	1.357	1.369
r(C2–C3)	1.354(48)	1.379(3)	1.391	1.377	1.382(9)	1.357	1.377
r(C1–C2)	1.321(63)	1.397(3)	1.371	1.395	1.393(8)	1.375	1.390
r(C1–C6)	1.577(27)	1.505(3)	1.497	1.503			
r(C–H <sub>ring</sub> )	1.040	1.086(3)	1.049	1.080	1.070	0.940	1.079
r(C–H <sub>methyl</sub> )	1.095	1.097(3)	1.033	1.091			
∠ C2NO	117.2(16)	121.2(8)	120.2	121.0	119.5	120.6	120.8
∠ NC3C2	115.9(11)	122.1(8)	120.6	121.5	118.1	120.9	121.4
∠ C3C2C1	121.0(29)	120.8(6)	121.0	121.6	124.4	120.7	120.6
∠ NC4H2	104.8	119.0(5)	118.7	113.9	120.5	109.3	113.8
∠ C3C2H1	115.9	119.6(5)	117.7	117.9	110.0	117.4	118.3
∠ C1C6H5	109.3	108.6(5)	114.1	111.2			
				111.4			
H6C6C1C2	34.5	32.4(67)		30.8			

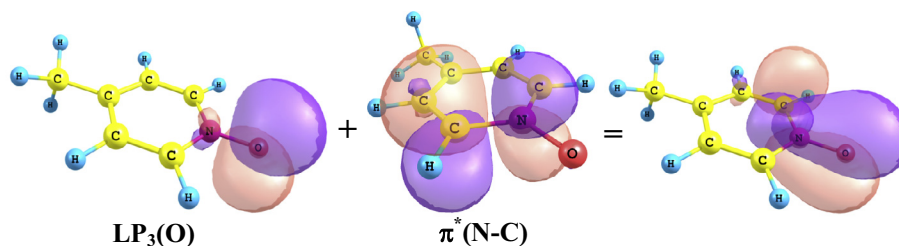


Fig. 4. The hyper conjugation between lone pair  $LP_3(O)$  of oxygen and antibonding  $\pi^*(N-C)$  in 4-MePyO.

type (bonds or lone pairs) NBO orbitals and formally unoccupied (antibonding) non-Lewis NBO orbitals corresponds to a stabilizing donor-acceptor interaction. The energy of these interactions can be estimated by the second order perturbation theory. Table 7 collects the largest values of calculated second order interaction energies ( $E^2$ ) between donor-acceptor orbitals in PyO and 4-MePyO. In both cases several values correspond to the interactions related to the resonance in the pyridine ring, i.e. the interactions between  $\pi(C-C)$  and  $\pi^*(C-C)$  and between  $\pi(C-C)$  and  $\pi^*(C-N)$ . The nature of semipolar N–O bond was explained in detail [18]. The largest second order interaction energies ( $E^2$ ) in both molecules correspond to the  $LP_3(O)$  interaction with the antibonding  $\pi^*(N-C)$  NBO (Fig. 4.). Such interaction can lead to partial transfer of electron density from  $LP_3(O)$  to the  $\pi$ -system of the pyridine ring. As the result, the occupancy of the  $LP_3(O)$  p $\pi$ -orbital of oxygen is only 1.62e or 1.65e in PyO and 4-MePyO, respectively.

To study the substituent effect on the aromaticity the nuclear independent chemical shifts NICS(1) have been calculated by using B3LYP/aug-cc-pVTZ approximation. NICS(1) values correspond to the negative isotropic shielding (in ppm) at 1 Å above the ring plane. The calculated values of NICS(1):  $-7.40$  (PyO) and  $-7.36$  (4-Me-PyO) are very close to each other. Thus, from the NICS(1) values one can conclude that the introduction of  $CH_3$  group does not noticeably affect the aromaticity of the pyridine-N-oxide. Furthermore, the data of Table 5 do not confirm the conclusion of the authors of [15] about changing the aromaticity with substitution, which was made by analyzing the average values of bond length in the pyridine ring.

## Acknowledgment

This work was supported by the Ministry of Education and Science of the Russian Federation (the project N 4.3232.2017/PP). The quantum chemical calculations have been performed with the financial support by Vietnam National University, Hanoi (VNU) under project number QG.17.37.

## References

- [1] H.T. Kyu, *Ab initio* SCF and CI study of the electronic spectrum of pyridine N-oxide, *Theor. Chem. Acc.* 43 (1977) 337–349.
- [2] K. Fukuhara, A. Hakura, N. Sera, H. Tokiwa, N. Miyata, 1- and 3-nitro-6-azabenzopyrenes and their N-oxides: highly mutagenic nitrated azaarenes, *Chem. Res. Toxicol.* 5 (1992) 149–153.
- [3] A. Albini, S. Pietra, *Heterocyclic N-oxides*, CRC, Boca Raton, 1991.
- [4] J. Balazarini, M. Stevens, E. de Clercq, D. Schols, C. Pannecouque, *J. Antimicrob. Chemother.* 55 (2005) 135.
- [5] J. Balazarini, M. Stevens, G. Andrei, *Pyridine oxide derivatives: structure-activity relationship for inhibition of human immunodeficiency virus and cytomegalovirus replication in cell culture*, *Helv. Chim. Acta* 85 (2002) 2961–2974.
- [6] J. Balazarini, E. Keyaerts, L. Vijgen, F. Fandermeer, M. Stevens, E. De Clercq, H. Egberick, M. van Ranst, *Pyridine N-oxide derivatives are inhibitory to the human SARS and feline infectious peritonitis coronavirus in cell culture*, *J. Antimicrob. Chemother.* 57 (2006) 472.
- [7] E. Ochiai, *Aromatic Amine Oxides*, Elsevier, Amsterdam, 1977.
- [8] S.P. Ponomarenko, Y.J. Borovikov, N.S. Pivovarova, G.S. Borovikova, V.P. Makoveckii, *Zh. Obshsh. Khim.* 53 (1993) 1872.
- [9] A. Teasdale (Ed.), *Genotoxic Impurities, strategies for Identification and Control*, Wiley, Hoboken, 2011.
- [10] H. Arata, M. Shimizu, K. Takamiya, Purification and properties of trimethylamine N-Oxide reductase from aerobic photosynthetic bacterium *roseobacter denitrificans*, *J. Biochem.* 112 (1992) 470–475.
- [11] K. Takekawa, S. Kitamura, K. Sugihara, S. Ohta, Non-enzymatic reduction of aliphatic tertiary amine N-oxides mediated by the haem moiety of cytochrome P450, *Xenobiotica* 31 (2001) 11–23.
- [12] K. Takekawa, K. Sugihara, S. Kitamura, K. Tatsumi, Nonenzymatic reduction of brucine N-oxide by the heme group of cytochrome P450, *Biochem. Mol. Biol. Int.* 42 (1997) 977–981.
- [13] V.P. Andreev, Electronic factors effects on the reactivity of heteroaromatic N-oxides, *Khim. Geterotsikl. Soed.* (2010) 227–242.
- [14] J.F. Chiang, Molecular structure of pyridine N oxide, *J.Chem. Phys.* 61 (1974) 1280–1283.
- [15] J.F. Chiang, J.J. Song, Molecular structures of 4-nitro-, 4-methyl- and 4-chloropyridine-N-oxides, *J. Mol. Struct.* 96 (1982) 151–162.
- [16] W. Clegg, G.M. Sheldrick, U. Klingebiel, D. Bentmann, G. Henkel, K. B, *Acta Crystallogr. Sect. C* 40 (1984) 819.
- [17] Y. Wang, R.H. Blessing, F.K. Ross, P. Coppens, *Acta Crystallogr. Sect. B* 32 (1976) 572.
- [18] N.V. Belova, N.I. Giricheva, M.S. Fedorov, Substituent effect on the properties of pyridine-N-oxides, *Struct. Chem.* 26 (2015) 1459–1465.
- [19] G.V. Girichev, A.N. Utkin, Y.F. Revichev, Upgrading the EMR-100 Electron-diffraction Camera for Use with Gases, *Instruments and Experimental Techniques*, vol. 27, 1984, pp. 457–461. New York.
- [20] G.V. Girichev, S.A. Shlykov, Y.F. Revichev, *Apparatus for Study of Molecular Structure of Valence-unsaturated Compounds, Instruments and Experimental Techniques*, vol. 29, 1986, pp. 939–942. New York.
- [21] M.J. Frisch, G.W. Trucks, H.B. Schlegel, G.E. Scuseria, M.A. Robb, J.R. Cheeseman, J.A. Montgomery Jr., J.T. Vreven, K.N. Kudin, J.C. Burant, J.M. Millam, S.S. Iyengar, J. Tomasi, V. Barone, B. Mennucci, M. Cossi, G. Scalmani, N. Rega, G.A. Petersson, H. Nakatsuji, M. Hada, M. Ehara, K. Toyota, R. Fukuda, J. Hasegawa, M. Ishida, T. Nakajima, Y. Honda, O. Kitao, H. Nakai, M. Klene, X. Li, J.E. Knox, H.P. Hratchian, J.B. Cross, C. Adamo, J. Jaramillo, R. Gomperts, R.E. Stratmann, O. Yazyev, A.J. Austin, R. Cammi, C. Pomelli, J.W. Ochterski, P.Y. Ayala, K. Morokuma, G.A. Voth, P. Salvador, J.J. Dannenberg, V.G. Zakrzewski, S. Dapprich, A.D. Daniels, M.C. Strain, O. Farkas, D.K. Malick, A.D. Rabuck, K. Raghavachari, J.B. Foresman, J.V. Ortiz, Q. Cui, A.G. Baboul, S. Clifford, J. Cioslowski, B.B. Stefanov, G. Liu, A. Liashenko, P. Piskorz, I. Komaromi, R.L. Martin, D.J. Fox, T. Keith, M.A. Al-Laham, C.Y. Peng, A. Nanayakkara, M. Challacombe, P.M.W. Gill, B. Johnson, W. Chen, M.W. Wong, C. Gonzalez, J.A. Pople, *Gaussian 03, Revision B.03*, Gaussian, Inc, Pittsburgh PA, 2003.
- [22] C.W. Bauschlicher, H. Partridge, Cr2 revisited, *Chem. Phys. Lett.* 231 (1994) 277–282.
- [23] A.D. Becke, Density-functional thermochemistry. III. The role of exact exchange, *J. Chem. Phys.* 98 (1993) 5648–5652.
- [24] A.D. Becke, Density-functional exchange-energy approximation with correct asymptotic behavior, *Phys. Rev. A* 38 (1988) 3098–3100.
- [25] C. Lee, W. Yang, R.G. Parr, Development of the Colle-Salvetti correlation-energy formula into a functional of the electron density, *Phys. Rev. B* 37 (1988) 785–789.
- [26] S.H. Vosko, L. Wilk, M. Nusair, Accurate spin-dependent electron liquid correlation energies for local spin density calculations: a critical analysis, *Can. J. Phys.* 58 (1980) 1200–1211.
- [27] C. Adamo, V. Barone, Toward reliable density functional methods without adjustable parameters: the PBE0 model, *J. Chem. Phys.* 110 (1999) 6158–6169.
- [28] V.A. Sipachev, Local centrifugal distortions caused by internal motions of molecules, *J. Mol. Struct.* 567–568 (2001) 67–72.
- [29] V.A. Sipachev, Calculation of shrinkage corrections in harmonic approximation, *J. Mol. Struct. (THEOCHEM)* 121 (1985) 143–151.
- [30] V.A. Sipachev, in: I. Hargittai, M. Hargittai (Eds.), *Advances in Molecular Structure Research*, JAI Press, New York, 1999, pp. 263–311.
- [31] E.D. Glendening, J. Badenhoop, K.A.E. Reed, J.E. Carpenter, J.A. Bohmann,

- C.M. Morales, F. Weinhold, NBO 5.G. 2004: Theoretical Chemistry Institute, University of Wisconsin, Madison, WI, 2004. <http://www.chem.wisc.edu/~nb05>.
- [32] A. A. Granovsky, PC GAMESS version 7.1 (Firefly): [www http://classic.chem.msu.su/gran/firefly/index.html](http://classic.chem.msu.su/gran/firefly/index.html).
- [33] G. A. Zhurko, D. A. Zhurko, ChemCraft version 1.6 (build 312), version 1.6 (build 312) ed: <http://www.chemcraftprog.com/index.html>.
- [34] E.K. Morris, A. Cousson, W. Paulus, Crystal structure of 4-methylpyridine N-oxide, C<sub>6</sub>H<sub>7</sub>NO, Z. Kristallogr.- New Cryst. Struct. 213 (1998) 80.
- [35] E. Patyk, J. Marciniak, H. Tomkowiak, A. Katrusiak, K. Merz, Isothermal and isochoric crystallization of highly hygroscopic pyridine N-oxide of aqueous solution, Acta Crystallogr. Sect. B Struct. Sci. 58 (2014) 62–77.
- [36] A. Domenicano, A. Vaciago, C.A. Coulson, Molecular geometry of substituted benzene derivatives. I. On the nature of the ring deformations induced by sublimations, Acta Cryst. B31 (1975) 221–234.
- [37] A.R. Campanelli, A. Domenicano, F. Ramondo, I. Hargittai, Group Electronegativities from benzene ring deformations: a quantum chemical study, J. Phys. Chem. A 108 (2004) 4940–4948.